ENGLACIAL RADAR ATTENUATION RATES IN THE PROMETHEI LINGULA AREA OF THE MARTIAN SOUTH POLAR LAYERED DEPOSITS. K. M. Scanlan, D. A. Young, C. Grima, G. Steinbrügge, S. D. Kempf and D. D. Blankenship, Institute for Geophysics, University of Texas at Austin, 10100 Burnet Road, Building 196, Austin, TX 78758.

Introduction: Mapping internal stratigraphic layers from SHARAD radargrams in the Martian south polar layered deposits (SPLD) provides key insight into the erosional and depositional processes shaping these features [1,2]. However, in contrast to layers the north polar layered deposits (NPLD), their distribution and appearance across the SPLD exhibits strong regional variation [3]. This regional variability in internal layer appearance and pervasiveness has been attributed to fluctuations in SHARAD signal scattering and attenuation within the SPLD [2].

In this study, we attempt to constrain englacial attenuation rates using 28 SHARAD USRDR radargrams in the Promethei Lingula area of the SPLD (Fig. 1). Promethei Lingula is selected due the clarity and continuity of SHARAD internal SPLD reflections in this region [1, 3]. Englacial attenuation rates are estimated from geometric spreading-corrected SHARAD radargrams following a procedure developed for terrestrial ice caps and glaciers [4]. Similar to [4], we assume that internal layer reflections within the SPLD are specular and that attenuation rates are constant during radar wave propagation through the ice column along individual range lines.

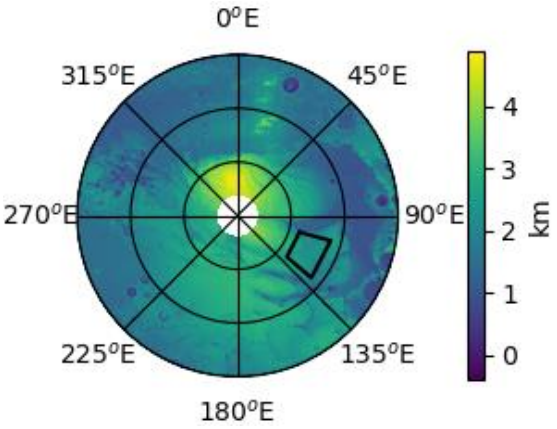

Fig. 1. MOLA basemap of the Martian south pole below 75°S latitude and the location of the area of interest (outlined in black) in Promethei Lingula.

Layer Selection in Promethei Lingula: Internal layers within the SHARAD radargrams are selected manually. Range samples that correspond to the internal layers are defined at the locations of the maximum signal amplitude within manually defined window. Fig. 2 presents the results of internal interface picking for the portion of SHARAD orbit 10562 in the area of interest. The radargram in Fig. 2 is displayed in power [dB] and has been geometrically-corrected using platform altitudes reported with the fully-processed US SHARAD data products and a subsurface SPLD dielectric permittivity of 3.4 [1]. The manual layer picking procedure is used to define the position of the surface echo as required for the geometric spreading correction [4].

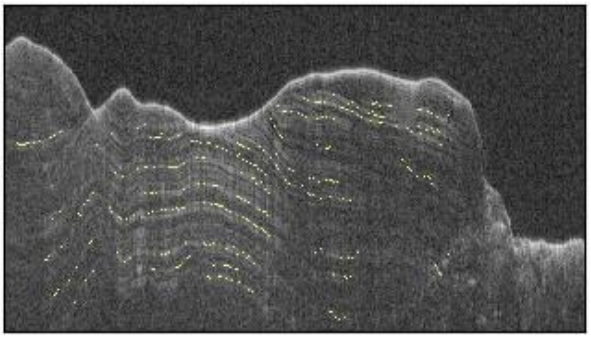

Fig. 2. Portion of SHARAD orbit 10562 with manually selected internal reflections. A conservative approach is followed during layer selection to mitigate against the mis-identification of sidelobes and off-nadir cross-track clutter as internal reflections.

Inspection of Fig. 2 reveals numerous additional signals within the SHARAD radargram that were not selected but exhibit similar character. A conservative approach to layer definition is taken in order to mitigate against the selection of features that may ultimately be related to two separate phenomena; 1) reflection sidelobes introduced during range compression [5, 6] and 2) off-nadir cross-track clutter.

Based on the uniform amplitude model for the SHARAD chirp that is used by the US processing team during data reduction, more prominent sidelobes in the SHARAD radargrams exist downrange of the actual interface reflections. Therefore, by defining internal layers near the start of dense bands of signal, such as are observed in Fig. 2, the potential for including sidelobes in attenuation rate estimation is minimized.

In addition to sidelobes, off-nadir cross-track clutter may also appear similar to reflections from internal layers within the SPLD, similar to what has been observed on Earth [7]. After manual layer picking, each

of the 28 radargrams used in this analysis is qualitatively compared with a simulated radargram based on spacecraft positions and MOLA [8]. Any picked interface that appears to be closely related to off-nadir cross-track signals in the simulated radargram is removed.

Calculation of Attenuation Rates: Once the internal layers have been defined, englacial attenuation rates are estimated using a procedure similar to one that has been implemented in terrestrial studies [4]. However, as the trace spacing along a particular SHARAD groundtrack (460m) is significantly coarser than for airborne datasets collected on Earth (1-10's of meters), the reflected powers along each interface were not binned into successive 1km-long segments. Instead an attenuation rate is estimated for each range line and the results smoothed using a 67 sample (30.82km) moving average. The 67 point moving average filter is one order of magnitude greater than the diameter of SHARAD's first Fresnel zone [4], considering a nominal platform altitude of 300km. Similar to [4], attenuation rates are only extracted from SHARAD traces when 5 or more internal layers have been selected.

Results and Discussion: The distribution of englacial attenuation rates derived from the 28 SHARAD groundtracks covering Promethei Lingula is presented in Fig. 3. Calculated attenuation rates vary between slightly greater than 0 and approximately 6.5dB/km with a large and prominent concentration between 4 and 5dB/km. These values fit within the range englacial on attenuation rates previously observed in the NPLD [9].

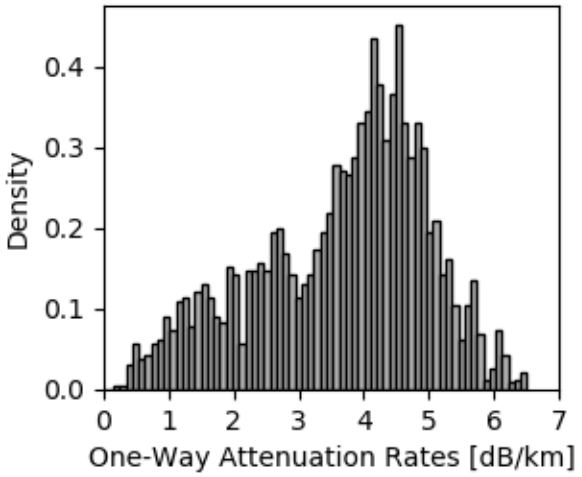

Fig. 3. Distribution of englacial attenuation rates derived from 28 SHARAD orbits in the Promethei Lingula region of the Martian SPLD.

While the englacial attenuation rates presented in Fig. 3 are smaller than those observed along the margins of terrestrial ice masses, attenuation rates in the interior can approach a similar level [4]. Considering ambient temperatures in the Martian polar regions can reach lows of 120K, overall low one-way englacial attenuation rates are not unexpected as the englacial attenuation rate increases with ice temperature.

In contrast to [9], the pattern of englacial attenuation rates (Fig. 3) does not appear to follow one single distribution but possesses a bi-modal or even tri-modal appearance. This is suggestive of spatial variability in the englacial attenuation rates across Promethei Lingula that may be related to fluctuations in ice temperature or composition. Continued analysis of additional SHARAD radargrams is be required to thoroughly investigate the possibility of spatial variability in one-way englacial attenuation rates.

The relatively low englacial attenuation rates calculated during this study of Promethei Lingula have important implications for the lack of visible internal layers across the SPLD as a whole. Low englacial attenuation rates should benefit internal layer visibility as less radar energy is lost during propagation through the ice column. Assuming conditions exist across the SPLD to generate pervasive internal reflections, similar to the NPLD, their absence from radargrams suggests one of two possibilities; 1) that englacial attenuation outside of Promethei Lingula is much stronger, or 2) signal scattering within Promethei Lingula is much weaker. Assuming the SPLD is similar to the NPLD and terrestrial ice masses, such as the Greenland Ice Sheet where attenuation rates increase toward the margin [4, 9], the existence of strong attenuation rates over a large area in the center of the SPLD is unlikely. It can then be inferred that signal scattering exerts an important control on radar sounding and internal layer detection across the SPLD and Promethei Lingula represents an area where it is particularly weak.

References: [1] Guallini, L., et al., *Icarus*, doi:10.1016/j.icarus.2017.08.030, 2017. [2] Putzig, N. E., et al., *Icarus*, doi:10.1016/j.icarus.2017.09.023, 2017. [3] Campbell, B. A., et al., #2366, 46th Lunar and Planetary Science Conference, 2015. [4] MacGregor, J. A., et al., *JGR*, 120, doi:10.1002/2014JF003418. [5] Campbell, B. A., et al., *IEEE Geoscience and Remote Sensing Letters*, 8, doi:10.1109/LGRS.2011.2143692, 2011. [6] Campbell, B. A., et al., *IEEE Geoscience and Remote Sensing Letters*, 11, doi:10.1109/LGRS.2013.2273396, 2014. [7] Holt, J. W., et al., *JGR*, 111, doi:10.1029/2005JE002525, 2006. [8] Zuber, M. T., et al., *JGR*, 97, doi:10.1029/92JE00341, 1992. [9] Grima, C., et al., *GRL*, 36, doi:10.1029/2008GL036326, 2009.